Phytochemistry Letters 3 (2010) 17–23

Contents lists available at ScienceDirect

Phytochemistry Letters

journal homepage: www.elsevier.com/locate/phytol

Short communication

Structure elucidation and an investigation into the *in vitro* effects of hop acids on human cancer cells

Elizabeth Tyrrell [a,*], Roland Archer [a], G.A. Skinner [a], Kuldip Singh [b], Kay Colston [c], Catherine Driver [c]

[a] School of Pharmacy, Kingston University, Penrhyn Road, Kingston, Surrey KT1 2EE, UK
[b] School of Chemistry, University of Leicester, Leicester, UK
[c] St George's University of London, Cranmer Terrace, London SW 17 0RE, UK

ARTICLE INFO

Article history:
Received 29 May 2009
Received in revised form 22 October 2009
Accepted 26 October 2009
Available online 26 November 2009

Keywords:
Natural and unnatural humulone
Apoptosis
Tautomerism
X-ray analyses
Lupulone
Colupulone
Major tautomer

ABSTRACT

An investigation into the keto-enol relationships in a number of hop acids has been undertaken. These provided samples to enable X-ray analyses of both natural **1** and unnatural humulone **5** to be carried out. Our results suggest that the configuration of humulone **1** may have been incorrectly assigned. An *in vitro* investigation into the biological activity of hop acids suggests that both humulone **1** and lupulone **2** exhibit significant activity against some human cancer cells. Our results provide evidence to show that they inhibit cell growth, induce caspase dependent apoptosis and inhibit adhesion of some cancer cells to bone tissue.

1. Introduction

Hops and malt have been used in the brewing process to provide the unique flavour and aroma associated with beer. During the evolution of the modern brewing industry it was found that hop extracts not only impart the taste to bitter ales but also are bacteriostatic (Kulka, 1958) in preventing the brew from spoiling (Simpson, 1993). Hop extracts contain a vast number of natural products however the principal compounds of interest in our investigations are (−)-(*R*)-humulone **1** and lupulone **2** both of which are isolated from an extract of the soft resins (Fig. 1).

The extensive pharmacognosy of hop isolates has been documented (Zanoli and Zavatti, 2008). In addition the anticollagen/antioxidant activity (Yamaguchi et al., 2009), anti-inflammatory activity (Hall et al., 2008), oestrogenic properties (Chadwick et al., 2006) and the inhibition of angiogenesis by **1** (Shimamura et al., 2001) serve to further emphasis their potential as therapeutic agents.

Our interest in **1** and **2** was initially focused upon increasing our understanding of their diverse chemistry however this has been extended to investigate their anti-cancer activity. The most intensively studied hop extract that exhibits this activity is xanthohumol (Stevens and Page, 2004) however humulone **1** either alone or as a mixture of hop bitters has been shown to inhibit cell proliferation (Gerhauser, 2005). Others have described the effects of lupulone **2** on human colon cancer derived metastatic cells (Lamy et al., 2007) and the *in vitro* activity of hexahydrocolupulone (Stephan et al., 1998). In this paper we would like to disclose the results from some fundamental studies that we have undertaken with hop isolates.

As part of our industrial remit initial investigations were focused upon the development of a method for obtaining unnatural (*S*)-(+)-humulone **5** both for evaluation and X-ray analysis. We have also studied the effects of solvents upon the tautomeric ratio of lupulone **2** and the structurally related progener colupulone **3**. The outcomes of these studies provided the first X-ray structures of the major tautomers of these compounds in polar solvents and hence provided some insight into any *in vivo* structure–activity relationship. Armed with this knowledge we, in association with our clinical collaborators, investigated the action of hop acids **1** and **2** on human cancer cells. We provide evidence to suggest that both humulone **1** and lupulone **2** inhibit cell growth and induce caspase dependent apoptosis. We conclude that both humulone **1** and lupulone **2** inhibit the adhesion of cancer cells to bone tissue.

2. Results and discussion

Much of our chemical understanding of hop acids is derived from pioneering studies conducted in 1970s (De Kerkeleire and

* Corresponding author. Tel.: +44 208 547 8810.
E-mail address: e.tyrrell@kingston.ac.uk (E. Tyrrell).

1874-3900/$ – see front matter © 2009 Published by Elsevier B.V. on behalf of Phytochemical Society of Europe.
doi:10.1016/j.phytol.2009.10.006

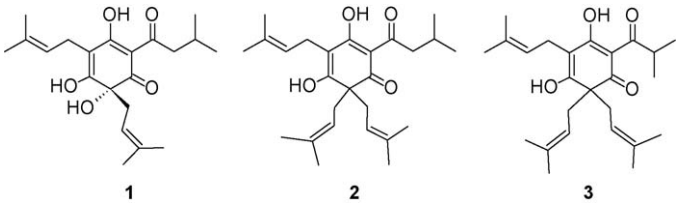

Fig. 1. Structures for (−)-(*R*)-humulone **1** (natural humulone), lupulone **2** and colupulone **3**.

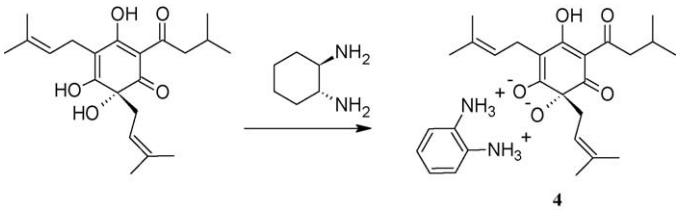

Fig. 2. Complexation of **1** with (1*R*, 2*R*)-(−)-diaminocyclohexane.

Verzele, 1970a,b; De Kerkeleire and Snatzke, 1972) and earlier (Verzele and Govaert, 1949) and to the best of our knowledge no X-ray or in-depth NMR studies of **1** or **2**, or their derivatives, have been undertaken. The configuration of the stereogenic centre in humulone **1** was assumed to be -(*R*) on the basis of chemical degradation studies (De Kerkeleire and Verzele, 1971). These assumed however that no scrambling in the stereochemistry occurred at the asymmetric centre. Results from our laboratories however place some doubt over the accuracy of this assignment.

Complexation of crude humulone extracts with *O*-phenylene diamine followed by multiple recystallisations of the solid complex from benzene has been the standard industrial method for purification of **1** (Clarke and Hildebrand, 1965). In our laboratories, however, we observed that exposure of (*R*)-(−)-humulone **1** to (1*R*, 2*R*)-(−)-diaminocyclohexane gave a complex **4** which proved to be completely insoluble in acetonitrile. In contrast exposure of **1** to (2*S*, 3*S*)-diaminocyclohexane provided a soluble derivative (Fig. 2).

We furthermore discovered that (*S*)-(+)-humulone **5** furnished a crystalline complex with (2*S*, 3*S*)-diaminocyclohexane which could be recrystallised from acetonitrile. Exploiting these differences in solubility between the two diamine complexes provided, for the first time, a new methodology for accessing mutigram quantities of unnatural (*S*)-(+)-humulone **5** for analysis. This was accomplished as follows: a crude liquid CO_2 extract of hops was heated in toluene until the optical rotation fell to zero as a result of racemisation. (+/−)-Humulone was isolated using the phenylene diamine complexation procedure which upon decomplexation gave (+/−)-humulone. Resolution of unnatural humulone **5** was then achieved *via* selective complexation with (1*S*, 2*S*)-(+)-diaminocyclohexane (Scheme 1).

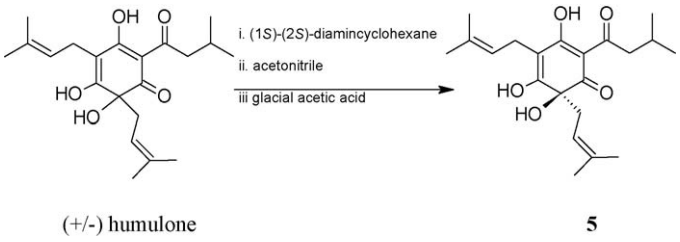

Scheme 1. The isolation of (*S*)-(−)-humulone **5**.

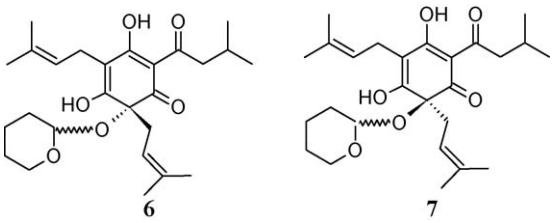

Fig. 3. O-THP ethers derivatives of humulones **1** and **5**.

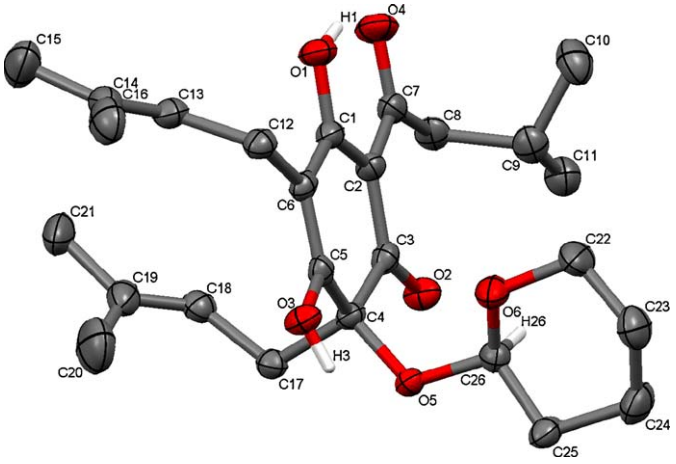

Fig. 4. X-ray structure for the O-THP-derivative **6** of humulone **1** shown as 50% thermal ellipsoids.

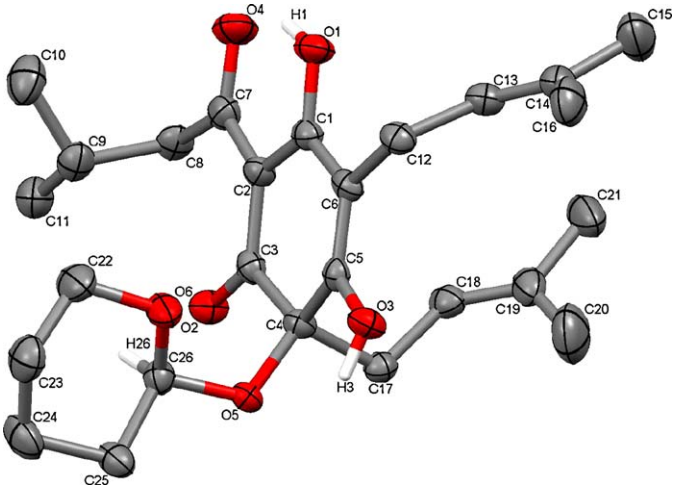

Fig. 5. X-ray structure for the O-THP-derivative **7** of humulone **5** shown as 50% thermal ellipsoids.

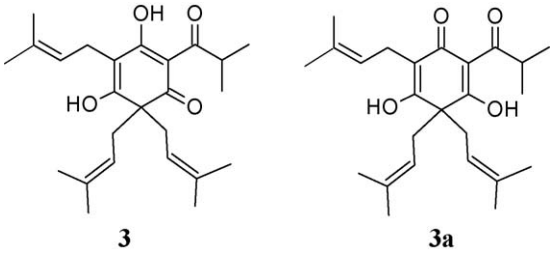

Fig. 6. Tautomers of colupulone.

As expected the resolved isolate exhibited a positive specific rotation (+244.98°) consistent with being the enantiomer to **1**. With both enantiomers of humulone **1** and **5** now in hand they were each derivatised in the hope that a crystalline derivative would be obtained for X-ray analysis and hence confirmation of structure. Our initial target was the O-THP ether derivatives which were formed to provide crystalline compounds with O-protection taking place in a regiospecific manner at the stereogenic tertiary C-4 hydroxyl group. The O-THP ethers **6** and **7** were formed from **1** and **5**, respectively each with a diastereoisomeric excess (de) of 20% however the major diastereoisomers were readily separable by chromatography on silica (Fig. 3).

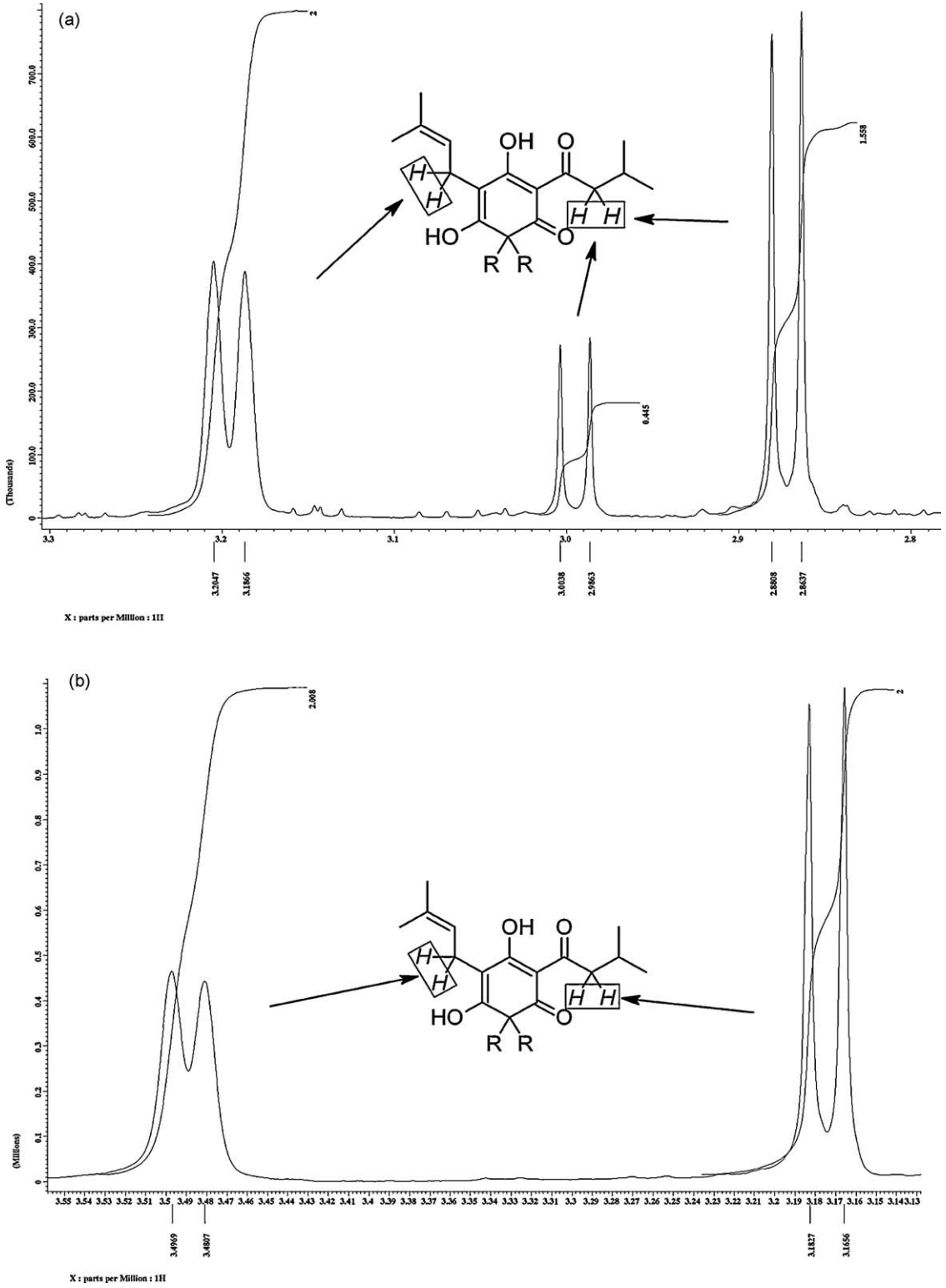

Fig. 7. (a) Part of the 400 MHz NMR of **2**/**2a** in d_{12} cyclohexane; (b) part of the 400 MHz NMR of **2**/**2a** in pyridine demonstrating the presence of one tautomer only.

X-ray quality crystals were obtained that provided the corresponding X-ray structure of compound **6**, the O-THP derivative of (*R*)-(−)-humulone **1** (Fig. 4) (Archer et al., 2007).

What becomes completely clear from this X-ray is that the configuration at the stereogenic centre, C-4 in compound **6** is (−*S*) whereas the X-ray obtained for the O-THP derivative **7** from unatural humulone **5** (Fig. 5) the configuration at C-4 is (−*R*).

As far as we have been able to ascertain no one has undertaken an investigation to either confirm or refute the configuration assigned to **1** over three decades ago and based upon degradation studies. Thus although the outcomes from these studies must remain tentative for the time being they are nevertheless noteworthy and serve to cast a doubt over the accuracy of the original assignment. From (Figs. 4 and 5) it can be seen that in fact derivatives **6** and **7** are related as enantiomers, i.e. **6** ((C4-(*S*), C26-(*R*)) with a specific rotation $\alpha_D = -127.78^\circ$ whereas for **7** ((C4-(*R*), C26-(*S*)) the $\alpha_D = +129.05^\circ$.

Hop isolates exhibit solvent dependant keto-enol tautomerism and it is noteworthy that few publications explicitly consider this important chemical characteristic (Payton et al., 2007; Sandusky, 2007). Colupulone **3** for instance exists in equilibrium with the tautomer **3a** in carbon tetrachloride. However, as far as we can ascertain, little is known about the *intra*molecular hydrogen bonding patterns of either tautomer or indeed whether one tautomer predominates at equilibrium (Fig. 6).

Using colupulone **3** and lupulone **2** we have carried out extensive ^{1}H NMR studies into this phenomena. Thus dissolution of **2** in a non-polar solvents such as toluene, cyclohexane or the chlorinated solvents a major tautomer predominates (70:30). In contrast, however, in polar solvents such as MeOH, CH_3COOH or DMSO one tautomer predominates (100:1). The tautomeric selectivity was readily demonstrated by the use of ^{1}H NMR spectroscopy. Focusing upon the methylene group of the C-2 acyl side chain in **2** in a d_{12} cyclohexane solution this resonance appears as a doublet, at δ 2.90 ppm (major tautomer) and δ 3.02 (minor tautomer) (Fig. 7a). In contrast the ^{1}H NMR spectrum of the same compound dissolved in pyridine is shown (Fig. 7b). The absence of a resonance at δ 3.02 ppm, attributed to the minor tautomer, confirms that only one tautomer is present. The two resonances clearly integrate for two protons each representing the two methylene groups present in this tautomer.

Having demonstrated, for the first time, the solvent conditions to ensure the formation of a single tautomer we used these conditions in order to obtain the first X-ray structures of lupulone **2**. A suitable sample was obtained by careful recrystallisation of **2** from acetic acid (Fig. 8).

These X-ray data clearly show the enolisation pattern of the major tautomer and the importance of *intra*molecular hydrogen bonding between C-1 hydroxyl and the C-7 carbonyl group. Geometric parameters concerning bond-lengths derived from the X-ray data confirm the association of these groups *via intra*molecular hydrogen bonding. Thus the bond length C5–O3 (C–O) was found to be 1.348 Å whereas for C3–O2 (C=O) the bond length is 1.239 Å. For the groups associated in hydrogen bonding we found the following C1–O1 1.301 Å and C7–O4 1.262 Å, i.e. intermediate in the magnitude of bond length between C–O and C=O. Molecular modeling was performed upon **2** (quantum CACHE CONFLEX/MM3) which confirmed that the tautomer shown (Fig. 8) was indeed 23 kcal mol^{-1} more stable than that between C-7 carbonyl and the C-3 hydroxyl, i.e. 50 kcal mol^{-1} and 73 kcal mol^{-1}. Using the same methodology we were also able to obtain the first X-ray structure of colupulone **3**. These data again confirm that stabilization of the major tautomer is achieved *via intra*molecular hydrogen bonding between C-1 hydroxyl and C-7 carbonyl (Archer et al., 2007).

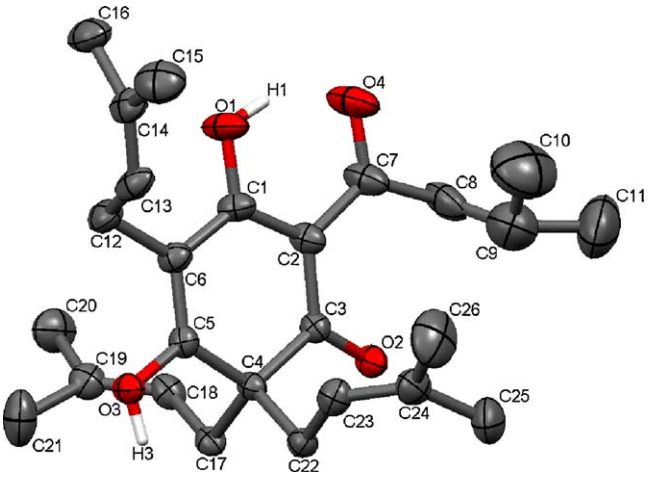

Fig. 8. X-ray structure for lupulone **2** shown as 50% thermal elipsoids.

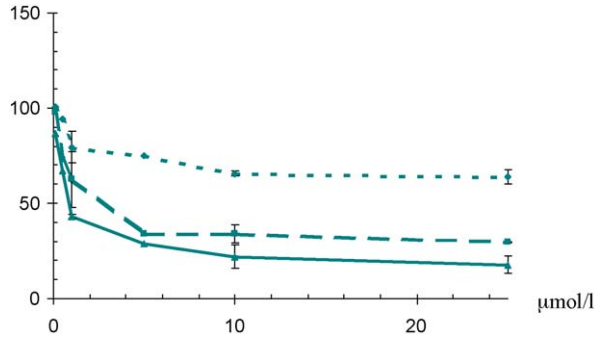

Fig. 9. The effects of lupulone **2** on growth of SK-MES lung cancer cells (legend upper = 24 h, middle = 48 h and lower = 72 h treatment. Graph shows residual cells as a function of concentration expressed as % control).

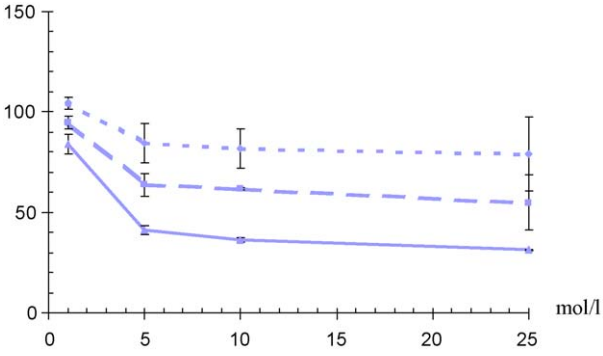

Fig. 10. The effects of lupulone **2** on growth of MDA-MB-231 breast cancer cells (legend: see Fig. 9).

To complement these studies we undertook some biological screening of **1** and **2**. The cell lines used for the assay were MDA-MB-231 (breast cancer) and SK-MES (lung cancer) (Driver et al., 2008) and initially we studied the potential of these hop isolates to inhibit cancer cell proliferation. Data from these experiments are shown in (Figs. 9–12).

These data suggest that the growth of both SK-MES and MDA-MB-231 cells was inhibited in a dose and time dependent manner by both **1** and **2**. A gradual decrease in viable cell numbers with time is apparent confirming a cytotoxic/cytostatic function in these hop isolates.

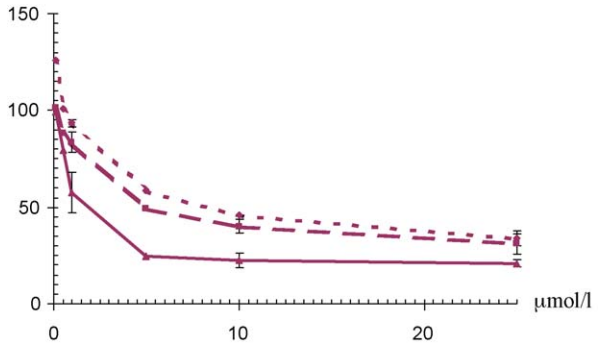

Fig. 11. The effects of humulone **1** on growth of SK-MES cells (legend: see Fig. 9).

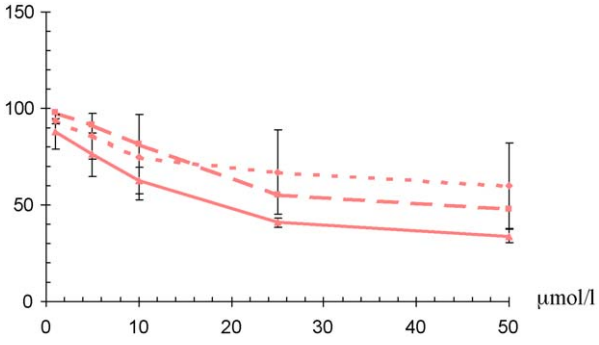

Fig. 12. The effects of humulone **1** on growth of MDA-MB-231 cells (legend: see Fig. 9).

In order to ascertain whether inhibition of cell growth was associated with the induction of apoptosis (active cell death) the Cell Death ELISA plus (Roche) to detect DNA fragmentation was used. The specific nucleotide enrichment of the sample was calculated as the ratio of absorbance, determined at 405 nm, of treated:control. This is the enrichment factor (EF) (Fig. 13).

Caspases are a group of calcium-dependant enzymes which play a significant role in apoptosis. Binding of an agonist to a relevant membrane receptor activates apoptosis. The broad-spectrum caspase inhibitor Z-VAD was used to assess the importance of caspase activation in cell death mediated by the hop acids **1** and **2**. These results suggest that exposure of SK-MES cells to **1** or **2** (24 h) induced significant DNA fragmentation suggesting cell death by apoptosis. Z-VAD is a synthetic peptide that irreversibly inhibits the activity of caspases and therefore blocks apoptosis. The results of these studies suggest that co-

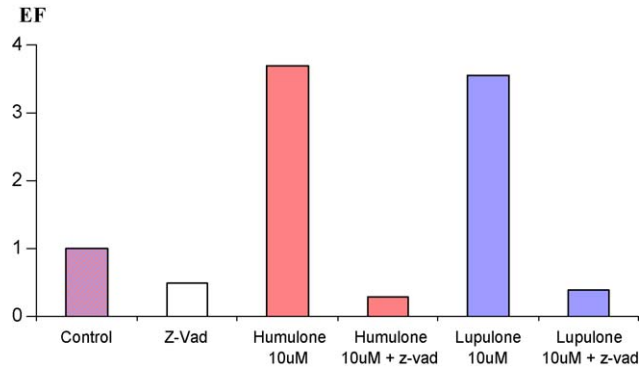

Fig. 13. The effects of hop acids and co-treatment with Z-VAD (a general caspase inhibitor) on induction of apoptosis (performed four times $n = 4$). An enrichment factor (EF) greater than 2 demonstrates significant apoptosis.

incubation with the caspase inhibitor Z-VAD rescued cells from apoptosis induced by both humulone **1** and lupulone **2**.

To conclude these studies the ability of hop acids to inhibit cell adhesion was investigated. The adherence of tumor cells is an important feature in proliferation and spreading of cancer to other regions of the body. The results show significant inhibition of adhesion of SK-MES cells to mineralised matrix following pre-treatment with 0.01 μM of humulone **1** (Fig. 14).

Matrigel™ mimics the constituents of basement membrane. The data suggest that pre-incubation with **2** significantly inhibits adhesion to Matrigel™ by a degree that appears similar to that seen with the bisphosphonate ADP (positive control) (Fig. 15).

Taken together our findings suggest that treatment of SK-MES cells with hop bitter acids, at a time and concentration that does not induce apoptosis leads to a significant inhibition of adhesion to both mineralised and non-mineralised matrices.

In conclusion we provide evidence to suggest that both humulone **1** and lupulone **2** inhibit cell growth and induce caspase dependent apoptosis. We provide data to suggest that both **1** and **2** inhibit adhesion of SK-MES and MDA-MB-231 cells to bone tissue. This final observation has important implications for processes that control the development of metastases. Wilcoxon signed ranks were used to determine statistical differences between controls and treated cells.

3. Experimental

3.1. General experimental procedures

HRMS was carried out by the EPSRC unit at Swansea using a Finnigan MAT900XL-QTrap VG Autospec. C,H,N microanalysis

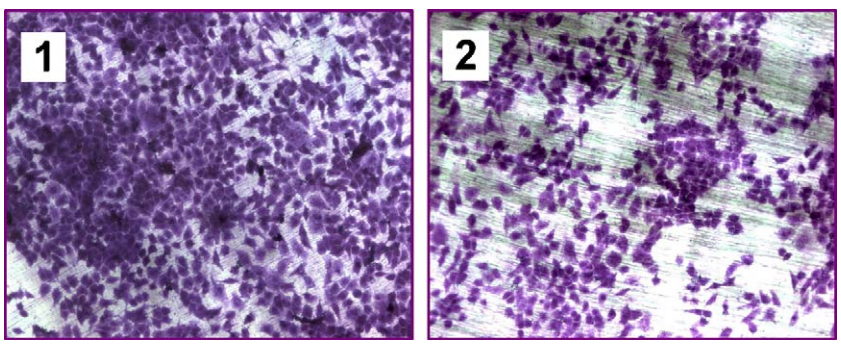

Fig. 14. SK-MES cell adhesion studies to dentine slices: (Picture 1) control—no humulone 1. (Picture 2) SK-MES pre-treated with 0.01 μM of humulone 1.

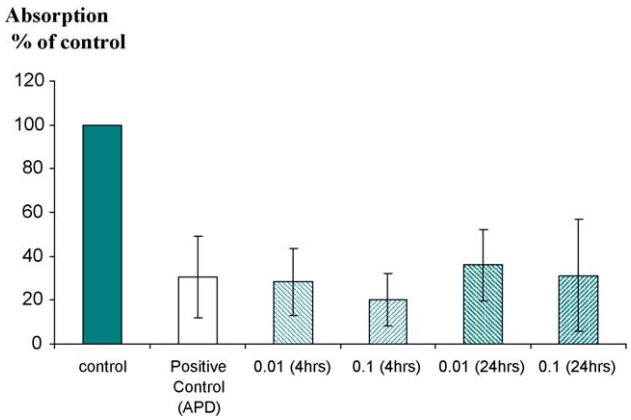

Fig. 15. The effects of pre-treatment with lupulone **2** 0.1 μM and 0.01 μM on adhesion of SK-MES cells to Matrigel™ (control = 100% adhesion).

from a Carlo-Erba EA 1108. IR spectra were performed on a Perkin Elmer 1 FT spectrophotometer. ^{1}H NMR spectra were obtained at 400 MHz using a JEOL Eclipse$^+$ 400 NMR spectrometer. Single crystal X-ray data was collected on a Bruker APEX 2000 diffractometer. Optical activity measurements were obtained with an AA-10 polarimeter.

3.2. Inhibition of cancer cell proliferation assay

Cancer cells were seeded into multiwell plates and incubated at 37 °C with increasing concentrations of either **1** or **2** for up to 72 h whereupon the cells were fixed, using 50% trichloroacetic acid, and cell protein stained with sulforhodamine B dye (Skehan et al., 1990). This dye binds to cellular proteins in the residual cell lines. After extensive washing, incorporated dye was eluted with 10 mM Trizma base and absorbance was determined at 550 nm using a Titertek plate reader.

3.3. Induction of apoptosis assay

The Cell Death ELISA plus (Roche) was used to detect DNA fragmentation. This contains antibodies specific for the 180 bp fragments of DNA produced by apoptosis and the histones around which this DNA is wrapped. The kit was used according to the manufacturer's recommendations. 1×10^3 SK-MES cells were seeded into a 96 well plate treated with 10 μM of **1** and **2** for 24 h. The cells were harvested and equal amounts of lysed cells were added into the Cell Death ELISA. The specific nucleotide enrichment of the sample was calculated as the ratio of absorbance determined at 405 nm of treated:control samples. This provided an enrichment factor (EF). Z-VAD, a synthetic peptide, irreversibly inhibits the activity of caspases and therefore blocks apoptosis. SK-MES cells, 1×10^3, were seeded and left overnight to adhere. The cells were then co-treated with Z-VAD (50 μM) and the hop acids (10 μM) for 24 h. Cell lysates were prepared and DNA fragmentation again ascertained by Cell Death ELISA.

3.4. Cell adhesion assay

SK-MES cells, pre-treated with 0.1 μM and 0.01 μM of **1** and **2** for 4 h and 24 h detached (non-enzymatically) from the culture flasks. They were then seeded (2×10^6) into 96 well plates onto either mineralised dentine slices or thinly coated with 1/1000 (12 μg/ml) dilution of Matrigel™ in serum free DMEM and incubated at 37 °C overnight. Adherent cells were stained with Crystal Violet dye, wash and incorporated stain eluted 100 μl solubilisation buffer (50/50 NaH_2PO_4, pH 4.5/50%. The absorbance was determined at 550 nm. Cells seeded onto dentine slices were incubated for 24 h, stained and counted.

3.5. Characterisation

3.5.1. (S)-3,4,6-Trihydroxy-4,6-bis-(3-methylbut-2-enyl)-2-(3-methylbutyryl)-cyclohexa-2,4-dienone **1b**

Mp 79.1–81.3 °C; $[\alpha]_D^{20}$ +244.98° (c = 0.5 $CHCl_3$); IR ν_{max} (ATR) 3356.1, 1666.3, 1622.74, 1517.80 cm^{-1}; ^{1}H NMR (CD_3OD) δ: 0.97 (3H, d, J = 6.72 Hz), 1.00 (3H, d, J = 6.72 Hz), 1.52, (3H, d, J = 0.94 Hz), 1.69 (6H, s), 1.73 (3H, d, J = 0.81 Hz), 2.14 (1H, sept., J = 6.72 Hz), 2.42 (2H, dd, J = 7.80, 13.96 Hz), 2.54 (1H, dd, J = 7.92, 13.96 Hz), 2.77 (2H, m), 3.03 (1H, dd, J = 7.12, 14.51 Hz), 3.11 (1H, dd, J = 7.12, 14.51 Hz), 4.17 (1H, broad s), 5.00 (1H, tm, J = 1.48, 7.92 Hz), 5.13 (1H, tm, J = 1.48, 7.25 Hz), 6.94 (1H,broad s); ^{13}C NMR (CD_3OD) δ: 17.90 (q), 18.03 (q), 21.22 (t), 22.68 (q), 22.94 (q), 25.89 (q), 26.15 (q), 26.58 (d), 45.16 (t), 46.32 (t), 78.83 (s), 106.15 (s), 109.43 (s), 115.86 (d), 121.11 (d), 132.98 (s), 138.37 (s), 167.68 (s), 191.04 (s), 195.17 (s), 200.01 (s).

3.5.2. (S)-3,5-Dihydroxy-4,6-bis-(3-methylbut-2-enyl)-2-(3-methylbutyryl)-6-[(R)-(tetrahydropyran-2-yl)-oxy]-cyclohexa-2,4-dienone **5**

Mp 96.6–99.4 °C; $[\alpha]_D^{20}$ +129.05° (c = 0.5 $CHCl_3$); Required: cC 69.93: H, 8.72% Found: C, 70.21; H, 8.92%. IR ν_{max} (ATR) 3175.32, 1656.76, 1623.86, 1514.50, 1455.15 cm^{-1}; ^{1}H NMR (CD_3OD) δ: 0.95 (3H, d, J = 6.58 Hz), 0.98 (3H, d, J = 6.72 Hz), 1.43–1.45, (2H, m), 1.49 (3H, d, J = 1.07 Hz), 1.73 (3H, s), 1.86 (1H, d, m), 2.00 (1H, m), 2.04 (1H, m), 2.13 (1H, sept., J = 6.72 Hz), 2.26 (2H, m), 2.74 (1H, dd, J = 6.58, 14.24 Hz), 2.92 (1H, dd, J = 7.52, 14.24 Hz), 3.06 (1H, dd, J = 6.58, 14.37 Hz), 3.13 (1H, dd, J = 7.39, 14.37 Hz), 3.40 (1H, m), 3.95 (1H, m), 4.38 (1H, dd, J = 2.42, 8.06 Hz), 4.95 (1H, tm, J = 1.34, 7.79 Hz), 5.12 (1H, tm, J = 1.34, 7.25 Hz), 7.68 (1H, s), 19.04 (1H,s); ^{13}C NMR (CD_3OD) δ: 17.79 (q), 17.94 (q), 21.44 (t), 21.54 (t), 22.81 (q), 22.9 (q), 24.92 (t), 25.92 (q), 26.05 (d), 31.66 (t), 41.48 (t), 47.32 (t), 66.36 (t), 86.61 (s), 100.17 (d), 108.47 (s), 115.98 (d), 121.54 (d), 132.58 (s), 137.58 (s), 167.27 (s), 190.33 (s), 192.68 (s), 201.32 (s). MS calcd. for C_{26} $H_{38}O_6$ 447.2741 $[M+H]^+$ found 447.2738.

Acknowledgements

We acknowledge the generosity of the BPSRG at Kingston University for financial support to RA, colleagues St Georges Hospital for their continued interest in this project and to the EPSRC Mass Spectroscopy service at the University of Swansea for providing an outstanding MS service.

References

Archer, R.P., Tyrrell, E., Singh, K., 2007. Acta Crystallogr. Sect. E E63, o1511–o1512 Compounds 1–3 contain atoms with weak scattering power which contribute to the Flack parameter. The X-ray structures are not absolute.
Chadwick, L.R., Pauli, G.F., Farnsworth, N.R., 2006. Phytomedicine 13, 119–131.
Clarke, B.J., Hildebrand, R.P., 1965. J. Inst. Brew. 71, 26–36.
De Kerkeleire, D., Verzele, M., 1970a. J. Inst. Brew. 76, 265–266.
De Kerkeleire, D., Verzele, M., 1970b. Tetrahedron 26, 385–393.
De Kerkeleire, D., Verzele, M., 1971. Tetrahedron 27, 4939–4945.
De Kerkeleire, D., Snatzke, G., 1972. Tetrahedron 28, 2011–2018.
Driver, C., Colston. K., 2008. MSc Project, St George's, London. The biological screening data was obtained by C. Driver as part of an MSc project. The choice of cell lines for screening for this project were based upon those available. The cell lines selected were different to those previously used by other workers in this area and so do provide some new data for consideration. The results obtained from these studies are preliminary and serve to complement the chemistry component of this paper. More in depth investigations are presently being carried out with a more diverse range of cancer cell lines and the results will be presented in due course.
Gerhauser, C., 2005. Eur. J. Cancer 41, 1941–1954.

Hall, A.J., Babish, J.G., Darland, G.K., Carroll, B.J., Konda, V.R., Lerman, R.H., Bland, J.S., Tripp, M.L., 2008. Phytochemistry 69, 1534–1547.
Kulka, D., 1958. J. Inst. Brew. 64, 331–337.
Lamy, V., Roussi, S., Chaabi, M., Gosse, F., Schall, N., Lobstein, A., Raul, F., 2007. Carcinogenesis 28, 1575–1581.
Payton, F., Sandusky, P., Alworth, W.L., 2007. J. Nat. Prod. 70, 143–146.
Sandusky, P., 2007. J. Nat. Prod. 70, 1895–1900.
Shimamura, M., Hazato, T., Ashino, H., Yamamoto, Y., Iwasaki, E., Tobe, H., Yamamoto, K., Yamamoto, S., 2001. Biochem. Biophys. Res. Commun. 289, 220–224.
Simpson, W.J., 1993. J. Inst. Brew. 99, 405–411.
Skehan, P., Storeng, R., Scudiero, D., Monks, A., McMahon, J., Vistica, D., Warren, J.T., Bokesh, H., Kenney, S., Boyd, M.R., 1990. J. Natl. Cancer. Inst. 82, 1107–1112.
Stephan, T.E., Ngo, E.O., Nutter, L.M., 1998. Biochem. Pharmacol. 55, 505–514.
Stevens, J.F., Page, J.E., 2004. Phytochemistry 65, 1317–1330.
Verzele, M., Govaert, F., 1949. Bull. Soc. Chim. Belg. 58, 432–438.
Wilcoxon signed ranks are the non-parametric equivalent of paired *t*-tests.
Yamaguchi, N., Satoh-Yamaguchi, Ono, M., 2009. Phytomedicine doi:10.1016/j.phymed 2008.12.021.
Zanoli, P., Zavatti, M., 2008. J. Ethnopharmacol. 116, 383–396.